

Prediction of Isotope Effects for Anticipated Intermediate Structures in the Course of Bacterial Denitrification

M. A. Morgenstern and R. L. Schowen

Department of Chemistry, University of Kansas, Lawrence, Kansas 66045-0046, USA

Z. Naturforsch. **44a**, 450–458 (1989); received January 10, 1989

This paper is dedicated to Professor Jacob Bigeleisen on the occasion of his 70th birthday

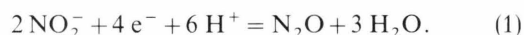
Vibrational-analysis methods have been used to estimate the equilibrium $^{14}\text{N}/^{15}\text{N}$ isotope effects to be expected for conversion of nitrite anion to thirteen possible intermediate-state and product-state structures [HONO, NO^+ , NO, NO^- , FeNO, ON* NO_2 , O* NNO_2 , O_2NNO_2 , ONO*N, O*NON, ONNO, * NNO , N* NO] in the reduction of nitrite ion to nitrous oxide denitrifying bacteria. The results, taken in combination with previous experimental isotope-effect and tracer studies of the *Pseudomonas stutzeri* and related systems, are consistent with a suggestion that a second nitrite anion enters the enzyme-catalytic cycle at the stage of a nitrosyl-ion intermediate but re-emerges after entry of the reducing electrons; the product nitrous oxide is then formed by disproportionation of enzymically generated hyponitrous acid. The calculations are consistent with contributions, under different experimental conditions, of several different transition states to limiting the rate of the enzymic reaction. These transition states (and the corresponding experimental conditions) are the transition states for N–O fission in the generation of a mononitrogen electrophilic species from nitrite anion (high reductant, high nitrite concentrations), for attack of nitrite on this electrophile (high reductant, low nitrite concentrations) and for electron transfer to a dinitrogen-trioxide-like species (low reductant concentration).

Introduction

The current period is witnessing the extension of isotope-effect techniques into ever more complex areas of biochemistry and biology. This development follows directly from the work of Professor Jacob Bigeleisen, summarized in his masterful 1958 review written with Max Wolfsberg [1]. This work links measured isotopic ratios of rate and equilibrium constants to molecular structures of reactant-state, transition-state and product-state molecules [2]. As the systems under experimental scrutiny become more complex, the advantages of isotope effects are still more emphatic, so that the technique is rapidly coming to dominate mechanistic biochemistry [3–5].

An extraordinary isotope-effect study of a very complex system has been reported by Bryan, Shearer, Skeeters, and Kohl [6]. They made use of the nitrogen kinetic isotope effect $J = k_{14}/k_{15}$ in the conversion of nitrite anion to nitrous oxide by cultures of the soil bacterium *Pseudomonas stutzeri*. They obtained essentially identical results with cell-free extracts, which

meant their findings were not determined by transport into the cells. The value of J was found to vary with the concentration of the substrate nitrite anion and with the concentration of the reducing agent succinate anion which were provided in the culture medium. The reaction under study was



The variation of J was linear in v/V , where v is the velocity under any particular conditions and V is the maximum velocity at saturating concentration of the reagent being varied. At a constant saturating value of $[\text{succinate}] = 25 \text{ mM}$, with $[\text{nitrite}]$ being varied, the value of J was 0.996 (SE 0.006) at $v/V = 0$ and 1.025 (SE 0.003) at $v/V = 1$ (largest experimental $[\text{nitrite}] = 2.2 \text{ mM}$). At $[\text{nitrite}] = 0.29 \text{ mM}$, J was 1.0036 (SE 0.0008) but rose as $[\text{succinate}]$ was decreased, reaching a value of 1.0142 (SE 0.0012) at $[\text{succinate}] \text{ ca. } 0.01 \text{ mM}$.

Several features of these results immediately attract attention. The fact that J varies with either $[\text{succinate}]$ or $[\text{nitrite}]$ indicates that the concentrations of these materials must be capable of shifting the importance of different possible rate-limiting steps in the catalytic sequence. Because these isotope effects are competitively measured effects, they must reflect isotope frac-

Reprint requests to Prof. R. L. Schowen, Department of Chemistry, University of Kansas, Lawrence, Kansas 66045-0046, USA.

0932-0784 / 89 / 0500-0450 \$ 01.30/0. – Please order a reprint rather than making your own copy.



Dieses Werk wurde im Jahr 2013 vom Verlag Zeitschrift für Naturforschung in Zusammenarbeit mit der Max-Planck-Gesellschaft zur Förderung der Wissenschaften e.V. digitalisiert und unter folgender Lizenz veröffentlicht: Creative Commons Namensnennung-Keine Bearbeitung 3.0 Deutschland Lizenz.

Zum 01.01.2015 ist eine Anpassung der Lizenzbedingungen (Entfall der Creative Commons Lizenzbedingung „Keine Bearbeitung“) beabsichtigt, um eine Nachnutzung auch im Rahmen zukünftiger wissenschaftlicher Nutzungsformen zu ermöglichen.

This work has been digitalized and published in 2013 by Verlag Zeitschrift für Naturforschung in cooperation with the Max Planck Society for the Advancement of Science under a Creative Commons Attribution-NoDerivs 3.0 Germany License.

On 01.01.2015 it is planned to change the License Conditions (the removal of the Creative Commons License condition “no derivative works”). This is to allow reuse in the area of future scientific usage.

Table 1. Geometric features and force constants used in BEBOVIB-IV calculations.

Molecule	Geometrical parameters (two-digit designations for bond distances; three-digit designations for bond angles; four-digit designations for torsions)	Force constants (mdyne/Å; mdyne-Å/rad ²); interaction constants in parentheses	Reference
Nitrite anion $\text{O}^1-\text{N}^2-\text{O}^3$	1, 2 = 1.24 Å 1, 2, 3 = 115	1, 2 = 7.57 1, 2, 3 = 2.48 (1, 2; 1, 2) = 2.08 (1, 2; 1, 2, 3) = 0.62	[10]
Nitrosonium cation O^1-N^2	1, 2 = 1.063 Å	1, 2 = 24.8	[10]
Nitric oxide O^1-N^2	1, 2 = 1.151 Å	1, 2 = 16.0	[10]
Monomeric hyponitrite anion O^1-N^2	1, 2 = 1.268 Å	1, 2 = 8.3	[10]
Symmetric dimeric nitric oxide $\text{O}^1-\text{N}^2-\text{N}^3-\text{O}^4$ (cis)	1, 2 = 1.12 Å 2, 3 = 21.8 Å 1, 2, 3 = 101 1, 2, 3, 4 = 0	1, 2 = 14.487 2, 3 = 0.323 1, 2, 3 = 0.340 1, 2, 3, 4 = 0.02 (1, 2; 1, 2, 3) = 0.111 (2, 3; 1, 2, 3) = 0.149 (1, 2, 3; 1, 2, 3) = 0.171 (1, 2; 1, 2) = 0.778 (1, 2; 2, 3) = -0.079	[11]
Asymmetric dimeric nitric oxide $\text{O}^1-\text{N}^2-\text{O}^3\text{N}^4$	1, 2 = 1.16 Å 3, 4 = 1.16 Å 2, 3 = 1.74 Å 1, 2, 3 = 107 2, 3, 4 = 107 (torsion omitted)	1, 2 = 12.77 3, 4 = 14.12 2, 3 = 1.02 1, 2, 3 = 0.163 2, 3, 4 = 0.122 (1, 2, 3; 2, 3, 4) = 0.032	[12]
Symmetric dinitrogen trioxide $\text{O}^1-\text{N}^2-\text{O}^3-\text{N}^4-\text{O}^5$ (trans, trans)	1, 2 = 1.20 Å 2, 3 = 1.46 Å 1, 2, 3 = 118 2, 3, 4 = 104 1, 2, 3, 4 = 0	1, 2 = 12.11 2, 3 = 3.61 1, 2, 3 = 1.61 2, 3, 4 = 1.87 1, 2, 3, 4 = 0.05 (1, 2; 2, 3) = 0.19 (1, 2; 2, 3, 4) = -0.39 (2, 3; 2, 3) = 0.36 (2, 3; 2, 3, 4) = 0.22 (2, 3; 1, 2, 3) = 0.16 (1, 2, 3; 1, 2, 3) = -0.16 (1, 2, 3; 2, 3, 4) = -0.33 (1, 2, 3, 4; 2, 3, 4, 5) = -0.01	[13] [14]
Asymmetric dinitrogen trioxide $\text{O}^1-\text{N}^2-\text{N}^3-\text{O}^4-\text{O}^5$	1, 2 = 1.142 Å 2, 3 = 1.864 Å 3, 5 = 1.202 Å 3, 4 = 1.217 Å 1, 2, 3 = 105.3 2, 3, 5 = 112.43 4, 3, 5 = 130.29 O, O, P = 0 1, 2, 3, 5 = 0	1, 2 = 15.04 2, 3 = 0.62 3, 5 = 9.574 3, 4 = 9.574 1, 2, 3 = 0.493 2, 3, 5 = 1.20 4, 3, 5 = 0.575 O, O, P = 1.30 1, 2, 3, 5 = 0.020 (1, 2; 2, 3) = 0.072 (2, 3; 3, 5) = 0.137 (2, 3; 3, 4) = 0.137 (3, 4; 3, 5) = 1.595 (3, 5; 4, 3, 5) = 0.541 (3, 4; 4, 3, 5) = 0.541 (2, 3; 2, 3, 5) = -0.175	[13] [15] [16]

Table 1. (Continued.)

Molecule	Geometrical parameters (two-digit designations for bond distances; three-digit designations for bond angles; four-digit designations for torsions)	Force constants (mdyne/Å; mdyne-Å/rad ²); interaction constants in parentheses	Reference
Nitrous oxide $\text{N}^1-\text{N}^2-\text{O}^3$	1, 2 = 1.128 Å 2, 3 = 1.184 Å 1, 2, 3 = 180	1, 2 = 18.48 2, 3 = 11.83 1, 2, 3 = 0.63 (1, 2; 2, 3) = 1.13	[10]
Iron-nitrosyl $\text{Fe}^1-\text{N}^2-\text{O}^3$	1, 2 = 1.77 Å 2, 3 = 1.12 Å 1, 2, 3 = 180	1, 2 = 5.07 2, 3 = 13.02 1, 2, 3 = 1.05	[17] [18] [19]
Nitrous acid $\text{H}^1-\text{O}^2-\text{N}^3-\text{O}^4$ (cis)	1, 2 = 0.96 Å 2, 3 = 1.46 Å 3, 4 = 1.21 Å 1, 2, 3 = 104 2, 3, 4 = 114 1, 2, 3, 4 = 0	1, 2 = 6.597 2, 3 = 4.364 3, 4 = 10.654 1, 2, 3 = 0.777 2, 3, 4 = 1.834 1, 2, 3, 4 = 0.162 (2, 3; 2, 3, 4) = 1.242 (3, 4; 1, 2) = 0.162	[20]

tiation before or during the first irreversible step in the catalytic sequence. Thus both [nitrite] and [succinate] must be able to shift the importance of different steps in limiting the rate within the manifold of steps before and at the first irreversible step. Finally, this means that the reductive donation of electrons originating in succinate anion must occur before or in the first irreversible step, not afterward.

The observation that J is larger than unity ("normal isotope effect") under many conditions is unsurprising for two reasons. First, the multiply bonded nitrogen in nitrite ion is in a very "stiff" binding state, i.e., in a "steep" potential well, so that transition states along the catalytic route might well have nitrogens in a looser or shallower potential well, thus contributing to a normal nitrogen isotope effect. Second, the formation or fission of bonds at nitrogen in the catalytic transition states could generate normal reaction-coordinate contributions, also tending to generate a normal overall isotope effect.

The perhaps surprising observation is then that under some circumstances (low values of [nitrite], high values of [succinate]) J becomes essentially equal to unity, or perhaps even slightly inverse (smaller than unity). An inverse isotope effect would signal transition states with binding at nitrogen even tighter than in nitrite anion; the same is true of a unit isotope effect

if it results from cancellation of an inverse binding effect with a normal reaction-coordinate contribution. Alternatively, a unit effect could signal a transition state with no reaction-coordinate contribution and binding at nitrogen identical to that in the initial nitrite anion.

It would obviously be advantageous to model the transition states by vibrational-analysis techniques [7] and to attempt to locate those that participate in the virtual transition states (weighted-average combinations of the actual transition states for individual steps in the reaction mechanism, when no single step truly limits the rate [8]) that dominate the reaction under various circumstances. Unfortunately, this is rendered extremely difficult by the necessary vagueness that currently attaches to the reaction mechanism. The reductase of *Pseudomonas aeruginosa* appears to be a cytochrome c, d_1 [9], but the enzyme is membrane-bound in vivo, is hard to isolate and may not possess the same kinetic characteristics in solution as in the native membranous state.

We have therefore concentrated on intermediate-state structures to which transition states might bear some resemblance. This necessarily leads to omission of all reaction-coordinate considerations, and the comparison of our estimates with experiment must be made with this limitation in mind.

Table 2. Calculated and observed frequencies.

Molecule	Calculated frequencies, cm^{-1} (observed in parentheses)	Reference for observed frequencies
Nitrite anion, NO_2^-	801 (809), 1237 (1240), 1318 (ca. 1320)	[21]
Nitrosonium cation, NO^+	2377 (2378)	[10]
Nitric oxide, NO	1908 (1904)	[10]
Monomeric hyponitrite anion, NO_2^-	1374 (1373)	[10]
Symmetric dimeric nitric oxide, N_2O_2	96 (97), 186 (187), 213 (214), 266 (266), 1761 (1762), 1866 (1866)	[11]
Asymmetric dimeric nitric oxide, N_2O_2 (torsion omitted)	118 (117), 186 (185), 487 (486), 1707 (1709), 1794 (1796)	[12]
Symmetric dinitrogen trioxide, N_2O_3	142 (140), 363 (366), 394 (395), 703 (704), 878 (877), 974 (973), 1687 (1687), 1743 (1740)	[13]
Asymmetric dinitrogen trioxide, N_2O_3	70 (70), 184 (205) ^a , 265 (266), 407 (405), 627 (627), 786 (784), 1281 (1288), 1592 (1590), 1857 (1859)	[13]
Nitrous oxide, N_2O	580 (596), 1299 (1298), 2283 (2283)	[10]
Iron-nitrosyl, FeNO [observed frequencies from $\text{Fe}(\text{CO}_2)(\text{NO}_2)$]	625 (619), 608 (654 [bend] or 614 [wag]), 1827 (1847)	[18]
Nitrous acid, HONO	616 (610), 636 (637), 853 (850), 1259 (1265), 1639 (1633), 3438 (3412)	[22]

^a This frequency shifts less than 0.1% for ^{15}N substitution in either site, so the discrepancy should not affect the calculated isotope effects.

Table 3. Calculated equilibrium nitrogen isotope effects at 298 K for conversion of nitrite anion to species along possible reaction pathways for bacterial denitrification.

Species	Mass/moment of inertia contribution MMI	Zero-point energy contribution, ZPE	Excited vibrational states contribution, EXC	K_{14}/K_{15}
Nitrous acid, HONO	1.0032	1.0015	0.9978	1.0025
Nitrosonium cation, NO^+	0.9737	1.0267	1.0010	1.0008
Nitric oxide, NO	0.9737	1.0478	1.0010	1.0213
Monomeric hyponitrite anion, NO_2^-	0.9737	1.0723	1.0009	1.0449
Iron-nitrosyl, FeNO	1.0344	0.9534	0.9915	0.9778
Asymmetric dinitrogen trioxide, $\text{ON}^{15}\text{NO}_2$	1.0367	0.9396	0.9918	0.9661
Asymmetric dinitrogen trioxide, $\text{O}^{15}\text{NNO}_2$	1.0228	1.0141	0.9763	1.0126
Symmetric dinitrogen trioxide, ONONO	1.0238	0.9854	0.9851	0.9938
Asymmetric dimeric nitric oxide, ONO^{15}N	1.0034	1.0450	0.9840	1.0318
Asymmetric dimeric nitric oxide, O^{15}NON	1.0135	1.0298	0.9902	1.0335
Symmetric dimeric nitric oxide, ONNO	1.0110	1.0338	0.9782	1.0224
Nitrous oxide, ^{15}NNO	0.9905	1.0159	0.9987	1.0050
Nitrous oxide, N^{15}NO	1.0251	0.9437	0.9925	0.9601

Methods of Calculation, Input Data and Calculated Frequencies

Vibrational-Analysis Procedure

The vibrational-analysis program BEBOVIB-IV of Sims and coworkers [7] was used. BEBOVIB-IV requires molecular geometries and force fields as input data and generates as output isotopic vibration frequencies, isotope effects and the components of the

effects arising from mass/moment-of-inertia (MMI) contributions, zero-point energy (ZPE) contributions and the contributions of excited vibrational states (EXC). The full BEBOVIB program includes the capacity to do calculations on transition-state models generated on a “bond-energy-bond-order” approach (thus BEBOVIB), but in this work, only the vibrational analysis parts were used in order to calculate equilibrium isotope effects.

Data for Calculations; Calculated Frequencies

The geometries and force constants for all species were taken from the literature; the values and references are given in Table 1. Observed and calculated vibration frequencies are shown in Table 2.

Results

The calculated equilibrium nitrogen isotope effects J at 298 K, for the conversion of nitrite anion to thirteen possible intermediate or product species in the denitrification pathway, along with their component contributions MMI, ZPE and EXC, are shown in Table 3.

Discussion

Previous Mechanistic Models

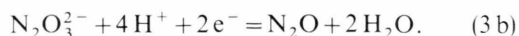
The previously discussed mechanisms for bacterial denitrification [6, 9, 23–25] have agreed on the initial conversion of nitrite to an electrophilic species such as $\text{Fe}^{\text{II}}-\text{NO}^+$, presumably formed by dehydration of a complex of nitrite anion with the heme-iron of the reductase. The mechanistic models have differed mainly with respect to how the N–N bond of the product NNO is formed.

The first type of mechanism [23] postulates the reduction of an intermediate like $\text{Fe}^{\text{II}}-\text{NO}^+$ to monomeric hyponitrous acid (HNO , “nitroxyl”), which then disproportionates to produce nitrous oxide:



This mechanism thus postulates the formation of two HNO molecules in *parallel* catalytic cycles of the enzyme, and it shall be referred to below as a *parallel mechanism*.

The second type of mechanism [24] postulates nucleophilic attack of a second nitrite anion on an intermediate like $\text{Fe}^{\text{II}}-\text{NO}^+$ to yield the equivalent of $\text{ON}-\text{NO}_2$ bound to the enzyme. This dinitrogen-trioxide-like species (“ON- NOO^+ ”) is then reduced to produce the trioxodinitrate dianion $\text{N}_2\text{O}_3^{2-}$, and the latter can form the product nitrous oxide:



In this mechanism, referred to as a “*serial mechanism*”, the product nitrous oxide is formed by *serial* reductions in a single catalytic cycle of the enzyme.

Each of the two types of mechanism is inconsistent with observations in the literature. The serial mechanism is inconsistent with a tracer experiment [25] and the parallel mechanism is inconsistent with isotope-effect experiments [6, 26].

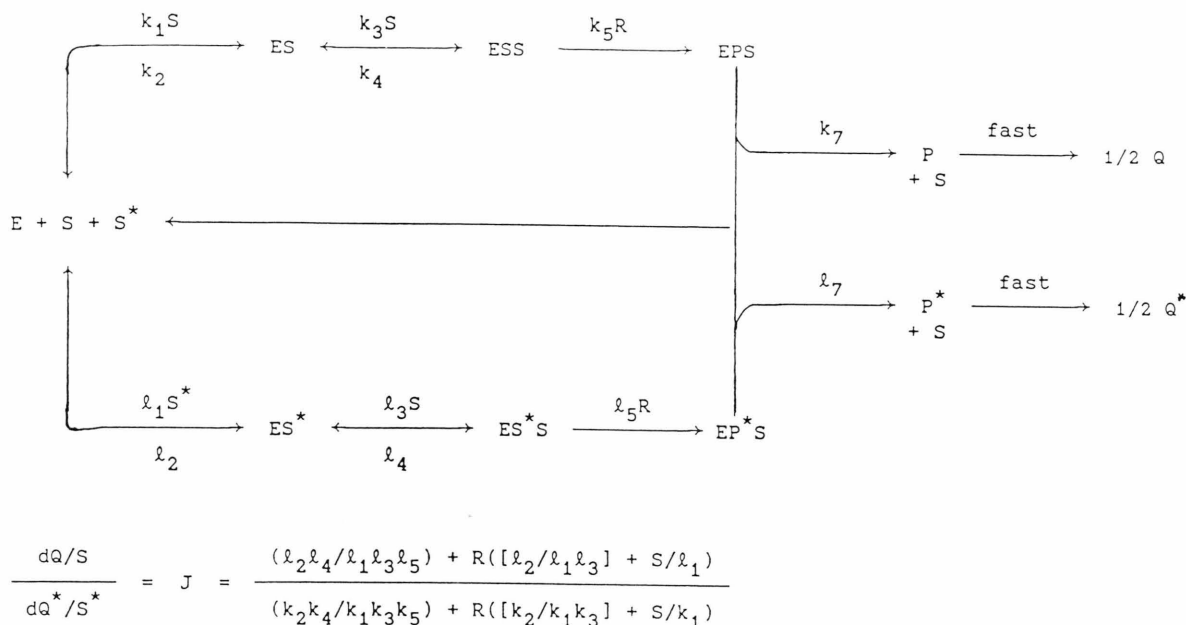
Inconsistency of the Serial Mechanism with Tracer Results

The serial mechanism as presented above is inconsistent with a tracer experiment of Garber, Wehrli, and Hollocher [25], who showed that the reaction of $^{15}\text{NO}_2$ in the presence of $^{14}\text{N}_2\text{O}_3^{2-}$ gave rise to the two mixed species $^{14}\text{N}^{15}\text{NO}$ and $^{15}\text{N}^{14}\text{NO}$. According to the serial mechanism, isotopically *unmixed* $^{15}\text{N}_2\text{O}$ would have been expected (at least very early in the reaction) if the added trioxodinitrate dianion could not intercept the enzyme and undergo the reaction (3 b). If the added trioxodinitrate dianion *can* intercept the enzyme then *unmixed* $^{14}\text{N}_2\text{O}$ would also be formed, at least early in the reaction. In no case, however, according to the serial mechanism, should the isotopically mixed nitrous-oxide product be formed. This isotopically mixed product, however, is in fact observed to form, even at very early points in the reaction. Such isotopically mixed products could arise in a parallel mechanism if the initial product HNO could isotopically mix, at least to some degree, with the trioxodinitrate dianion.

This tracer study, which was taken to exclude trioxodinitrate dianion as a reaction intermediate in denitrification, has been criticized on various grounds [26, 27]. We shall endeavor, however, to formulate a mechanism consistent with these findings, taken at their face value.

Inconsistency of the Parallel Mechanism with Isotope-Effect Results

The parallel mechanism as presented above is inconsistent with the observation of Bryan, Shearer, Skeeters, and Kohl [6] and of Shearer and Kohl [25] that the nitrogen isotope effect J varies with nitrite-anion concentration. According to the parallel scheme, nitrite-anion concentration cannot influence the degree to which different steps in the reaction sequence limit the rate, since nitrite anion enters the



sequence only once, in the initial step. There is therefore no means by which the parallel mechanism can account for the variation of J from around unity at infinitesimal concentrations to 1.025 at saturating concentrations of nitrite anion. On the other hand, a serial mechanism can readily account for this finding. High concentrations of nitrite anion will render the second addition step essentially irreversible, so that steps before this second addition must determine the rate and thus the value of J . Low concentrations of nitrite anion will make the second addition step (which is first-order in nitrite anion) correspondingly slow relative to preceding steps, and thus steps following the second addition may participate in limiting the rate at low nitrite-anion concentrations.

A Serioparallel Mechanism

The Chart shows a mechanism which combines parallel and serial characteristics to produce a mechanism consistent with both the tracer experiments and the isotope-effect experiments. It also appears to be consistent with reasonable transition-state structures, as indicated by a comparison of the equilibrium isotope effects presented in Table 3 with the experimental values of the kinetic isotope effect J obtained by Bryan, Shearer, Skeeters, and Kohl [6]. In the Chart, the enzyme E is shown in the competitive situation

employed in the experiments, capable of combining with ^{14}N -labeled nitrite anion S or ^{15}N -labeled nitrite anion S^* . The rate constants for the light-isotope pathway are designated by k 's, those for the heavy-isotope pathway by ℓ 's. For the purposes of the present discussion, the species ES and ES^* may be regarded as the electrophilic iron-nitrosyl or iron-nitrosonium compounds.

According to the Chart, a second nitrite anion adds to form the species ESS (or ES^*S ; with natural-abundance label; the formation of ES^*S^* can be neglected), which has the properties of "ON—NOO" mentioned above, in particular the capacity to accept electrons from the reductant. In contrast to its role in the previously-discussed serial mechanism, however, the nitro group of "ON—NOO" here serves simply as a conduit for the reductive electrons, so that the result of the reduction is the formation of a complex Fe—HNO—NO_2^- . The N—N bond of nitrous oxide is therefore not permanently formed at this stage, although an N—N bond may exist in the complex ESS . In the final step, the regenerated nitrite anion is released and the reduced product, which is also released at this point, is HNO (called P or P^*). This then generates nitrous oxide (Q or Q^*) by disproportion with a second molecule of HNO emerging from a parallel catalytic cycle of the enzyme (note that at natural-abundance levels of ^{15}N , P will always give Q

and P^* will give Q^*). This mechanism is therefore capable of accounting for the formation of isotopically mixed nitrous oxide from isotopically pure nitrite anion and trioxodinitrate dianion if it is assumed that HNO can mix with trioxodinitrate dianion [25].

The mechanism of the Chart can also account for the dependence of the isotope effect J on the concentrations of nitrite anion S and succinic-acid reductant R . Application of the steady-state hypothesis leads to the expression for J shown in the Chart, which can also readily be justified in conceptual terms. At very low reductant concentrations, steps at or after the reduction step determine the rate and thus the isotope effect ($R=0$ in the expression for J). In the Chart, the reduction step itself is taken as irreversible for purposes of simplification. The only alteration which would be occasioned by permitting a reversible reduction would be to include the product release step along with the reduction step in determining the isotope effect at very low reductant concentrations. At high reductant concentrations (R very large in the expression in the Chart), J becomes independent of R because the reduction step becomes so rapid as to render the preceding step irreversible. J remains dependent on S , the nitrite-anion concentration, however, as is observed experimentally for saturating reductant concentrations. At low S ($S=0$ in the expression), steps during the addition of the second nitrite anion should be rate-limiting and thus determine the isotope effect. At high S , steps preceding the second addition are rate-limiting and determine the isotope effect.

Chemical and Biological Rationality of the Serioparallel Mechanism

The mechanism of the Chart therefore can account for both the tracer and the isotope-effect observations. Its chief characteristic is that, although it postulates the addition of a second nitrite anion during the catalytic cycle (allowing a nitrite-anion concentration dependence for the isotope effect), it postulates that this nitrite anion is re-expelled unchanged, that the product of each cycle is HNO and that the product forms by disproportionation of this species.

It is logical to inquire about the biological economy of such a process, in which a second nitrite anion is first taken up and later re-expelled. In fact, there are good chemical and biological reasons why this might happen.

From a chemical point of view, it is entirely possible that the electrophilic iron-nitrosyl species might be more difficult to reduce than a species linked to the external environment by a nitro group, even though the latter brought negative charge with it. In effect, the nitro group, by providing a conduit for electron transfer, could well circumvent a sizable kinetic barrier to reduction at some thermodynamic cost produced by the negative charge.

From a biological point of view, the involvement of the second nitrite anion will generate a sigmoid character of the rate/concentration profile, making the system more responsive to the nitrite-anion concentration and achieving a sharper degree of control. This kind of regulation is similar to that seen in yeast pyruvate decarboxylase [28], where the enzyme must be activated by one molecule of pyruvate anion in order to catalyze decarboxylation of a second. Here, the enzyme must be activated by a second molecule of nitrite anion in order to catalyze reduction of the first.

Comparison of Estimated Equilibrium Isotope Effects with Possible Transition-State Structures: Principles

The spirit of the present approach derives from the work of Hartshorn and Shiner [29] and Buddenbaum and Shiner [30], who recognized the value of equilibrium isotope-effect calculations for the interpretation of mechanistic data. There are three points of comparison between the calculations and the experimental isotope effects. In all cases, the effects are competitive effects, so that the initial state is the free nitrite anion. The transition states for the three points of comparison are (refer to the Chart):

Condition of saturating R , saturating S :

$$J = [k_1]/[l_1] = 1.025.$$

Transition states between free nitrite anion/free enzyme and the transition state just preceding that for arrival of the second nitrite anion; included therefore are binding of the first nitrite anion, and the various steps of dehydration to generate the electrophilic iron-nitrosyl/nitrosonium species.

Condition of saturating R , very dilute S :

$$J = [k_1 k_3/k_2]/[l_1 l_3/l_2] = 0.996.$$

Transition states after arrival of the second nitrite anion but preceding arrival of the reductant, including

binding of the second nitrite anion and generation of the species "ON–NOO."

Condition of very dilute R:

$$J = [k_1 k_3 k_5 / k_2 k_4] / [l_1 l_3 l_5 / l_2 l_4] = 1.015.$$

Transition states after arrival of the reductant and up to product release or another irreversible step. Note that on the model of the Chart, the value of J at very dilute R is independent of S .

In all of these cases, it should be kept in mind that the rate constants defining J are composite constants of unknown composition, so that the transition states may be in principle either actual, single transition states or the weighted averages of more than one transition state (virtual transition states). A further matter for attention relates to the fact that a comparison is to be made of experimental kinetic isotope effects with theoretical estimates for equilibrium isotope effects for the formation of possible reaction intermediates. Therefore the experimental and theoretical values could disagree either because the structures of the transition states and the intermediates are different, or because the reaction-coordinate contribution to the experimental isotope effect is not included in the theoretical estimate. The reaction-coordinate contribution will always be "normal", favoring the light-isotopic species. Therefore, the disagreement from this source can only give rise to an experimental effect which is larger than the theoretical estimate.

At least a rough estimate of the probable magnitude of a reaction-coordinate contribution can be obtained by calculating the simple diatomic isotopic reduced-mass ratio for a typical heavy-atom (say, oxygen) bond to isotopic nitrogen. This is given by

$$\text{RCC} = \{[(1/14) + (1/16)] / [(1/15) + (1/16)]\}^{1/2} = 1.0183.$$

The Effect $J=1.025$ at Saturating R , Saturating S

J is determined by a virtual transition state consisting of any or all of the transition states between and including that for the arrival of the first nitrite anion and preceding that for arrival of the second nitrite anion. The relatively large effect of 1.025 excludes complete rate-limitation by transition states for diffusion or a simple binding (for both of which $J=1.000$). Also excluded are a single transition state not involving bond-breaking or bond-making to N (such as a

transition state for an enzyme conformational change) and resembling HONO-like species ($J=1.0025$, Table 1), the nitrosonium cation (1.008), monomeric hyponitrite anion (1.0449) or iron-nitrosyl (0.9778). A transition state of this type resembling nitric oxide is permitted (1.0213, which is sufficiently close to the observed effect that this structure ought not to be excluded). Also excluded are virtual transition states formed of any of the above (except for monomeric hyponitrite anion) and other transition states, such as that for binding, with $J=1.000$. A transition state resembling monomeric hyponitrite anion could be combined with one having $J=1.000$ in a virtual transition state with about equal contributions from each ($[1/2][1.045 + 1.000] = 1.023$, near the observed value).

Transition states resembling these species but also involving bond-making or bond-breaking at nitrogen would have a reaction-coordinate contribution, estimated above as around 1.018. This would permit single transition states of this type resembling HONO (1.021), perhaps nitrosonium cation (1.019), but would exclude those resembling iron-nitrosyl (0.996). Virtual transition states in which these three are the only contributors with non-unit J are also excluded, since the three isotope effects are equal to or smaller than the experimental effect. A single transition state of this type resembling nitric oxide is excluded (1.040) unless the reaction-coordinate contribution were nearly unity.

The allowed structures are strongly consistent with recent evidence [26, 27] that little reversal back to nitrite anion from states following $N-O$ bond fission occurs (lack of ^{18}O exchange from water into nitrite anion). The most reasonable hypothesis for the main rate-limiting transition state would seem to be one of the structures for $N-O$ fission to generate the electrophilic mononitrogen species.

The Effect $J=0.996$ at Saturating R , Low S

Contributing transition states here must be at or after arrival of the second nitrite anion and before arrival of the reductant. On the hypothesis that the second nitrite anion redissociates unchanged after the reduction step, only species with label in the nitrogen derived from the first nitrite anion need be considered. Any mononitrogen transition-state structures that generate an approximately unit equilibrium isotope effect might be considered, with an as-yet unbonded nitrite anion approaching: for example, a nitrosoni-

um-cation structure (1.008). Also, an iron-nitrosyl structure with the N—N bond in the process of forming ($0.9778 \times 1.018 = 0.996$) would be acceptable. On the other hand, a "late" transition state for N—N bond formation, resembling O^*NNO_2 (1.0126) can probably be excluded.

The Effect $J=1.014$ at Low R

The mechanism of the Chart holds that this effect will be independent of nitrite-anion concentration and will be determined by transition states during (or in a more general formulation during or after) reduction. The most interesting possibility here is probably O^*NNO_2 , which generates an equilibrium isotope effect of 1.0126, very close to the observation. The electron-transfer reaction is unlikely to generate any reaction-coordinate isotope effect, so this structure is consistent with the reduction step itself as rate-limiting.

Conclusions

It is still too early to draw definite conclusions in this complex system. It is, however, true that the

mechanism of the Chart is consistent with tracer and isotope-effect data currently available and with the further refinements that the rate before arrival of the second nitrite anion is chiefly determined by N—O bond fission to generate an electrophilic mononitrogen species, the rate after arrival of the second nitrite anion is chiefly determined by N—N bond formation (later to be reversed) and the rate after reductant arrival is chiefly determined by electron transfer in a transition state resembling dinitrogen trioxide.

Acknowledgements

It is a pleasure to offer our thanks to Professor Jacob Bigeleisen for his seminal contributions to the theory and practice of isotope-effect science, contributions which underlie all work of this kind. We are further extremely grateful to Georgia Shearer and Danny Kohl for calling our attention to the problems treated herein and for expending countless hours of patient instruction on our behalf. This work was supported by the National Institutes of Health and the University of Kansas General Research Fund.

- [1] J. Bigeleisen and M. Wolfsberg, *Adv. Chem. Phys.* **1**, 15 (1958).
- [2] L. Melander and W. H. Saunders, Jr., *Reaction Rates of Isotopic Molecules*, Wiley-Intersci., New York 1980.
- [3] W. W. Cleland, M. H. O'Leary, and D. B. Northrop, eds., *Isotope Effects of Enzyme-Catalyzed Reactions*, University Park Press, Baltimore 1977.
- [4] R. D. Gandour and R. L. Schowen, eds., *Transition States of Biochemical Processes*, Plenum Press, New York 1978.
- [5] M. H. O'Leary, *Ann. Rev. Biochem.* **1988**, 57, in press.
- [6] B. A. Bryan, G. A. Shearer, J. L. Skeeters, and D. H. Kohl, *J. Biol. Chem.* **258**, 8613 (1983).
- [7] L. B. Sims and D. E. Lewis, *Isot. Org. Chem.* **6**, 161 (1984).
- [8] R. L. Schowen, Chapter 2 in [4].
- [9] C.-H. Kim and T. C. Hollocher, *J. Biol. Chem.* **259**, 2092 (1984).
- [10] J. J. Laane and J. R. Olsen, *Progr. Inorg. Chem.* **27**, 465 (1980).
- [11] E. M. Nour, L.-H. Chen, M. M. Strube, and J. J. Laane, *J. Phys. Chem.* **88**, 756 (1984).
- [12] J. R. Olsen and J. J. Laane, *J. Amer. Chem. Soc.* **100**, 6948 (1978).
- [13] E. M. Nour, L.-H. Chen, and J. J. Laane, *J. Phys. Chem.* **87**, 113 (1983).
- [14] E. L. Veretti, *J. Mol. Struct.* **53**, 275 (1979).
- [15] A. H. Brittain, D. A. Cox, and R. L. Kuczkowski, *Trans. Faraday Soc.* **65**, 1963 (1969).
- [16] The force field was modified from that of [13] to improve the fit of calculated to observed frequencies.
- [17] L. O. Brockway and J. S. Anderson, *Trans. Faraday Soc.* **33**, 1233 (1937).
- [18] A. Poletti, A. Suntucci, and A. Foffani, *J. Mol. Struct.* **3**, 311 (1969).
- [19] The mass of iron was taken to be 56 amu.
- [20] M. Stern, W. Spindel, and E. U. Monse, *J. Chem. Phys.* **48**, 2908 (1968).
- [21] R. E. Weston and T. F. Brodsky, *J. Chem. Phys.* **27**, 683 (1957).
- [22] W. A. Guillory and C. A. Hunter, *J. Chem. Phys.* **54**, 598 (1971).
- [23] E. A. E. Garber and T. C. Hollocher, *J. Bio. Chem.* **257**, 8091 (1982).
- [24] B. A. Averill and J. M. Tiedje, *FEBS Lett.* **138**, 8 (1982).
- [25] E. A. E. Garber, S. Wehrli, and T. C. Hollocher, *J. Biol. Chem.* **258**, 3587 (1983).
- [26] G. Shearer and D. H. Kohl, *J. Biol. Chem.* **263**, 13231 (1988).
- [27] E. Weeg-Aeressens, J. M. Tiedje, and B. A. Averill, *J. Amer. Chem. Soc.* **110**, 6851 (1988).
- [28] J. Ullrich and I. Donner, *Hoppe-Seyler's Z. physiol. Chem.* **351**, 1026 (1970); A. Boiteux and B. Hess, *FEBS Lett.* **9**, 293 (1970); G. Hübner, G. Fischer, and A. Schellenberger, *Z. Chem.* **11**, 436 (1970).
- [29] S. R. Hartshorn and V. J. Shiner, Jr., *J. Amer. Chem. Soc.* **94**, 9002 (1972).
- [30] W. E. Buddenbaum and V. J. Shiner, Jr., In: Cleland, O'Leary and Northrop, Ref. [3], p. 1.